Nonlocal heat flux application for Scrape-off Layer plasma

Hugo Bufferand, G. Ciraolo, P Di Cintio, N Fedorczak, Ph Ghendrih, S. Lepri, R. Livi, Yannick Marandet, E. Serre, P. Tamain

Nonlocal heat flux application for Scrape-off Layer plasma

H. Bufferand[1,*], **G. Ciraolo**[1], **P. Di Cintio**[2], **N. Fedorczak**[1], **Ph. Ghendrih**[1], **S. Lepri**[2], **R. Livi**[3], **Y. Marandet**[4], **E. Serre**[5], and **P. Tamain**[1]

[1] IRFM-CEA F-13108 Saint-Paul-Lez-Durance, France
[2] CNR Florence, Italy
[3] University of Florence, Italy
[4] PIIM-CNRS, Marseille, France
[5] M2P2-CNRS, Marseille, France

Received XXXX, revised XXXX, accepted XXXX
Published online XXXX

Key words Plasma physics, heat conduction, non-local transport

The nonlocal expression proposed by Luciani-Mora-Virmont is implemented into a 1D fluid model for the scrape-off layer. Analytic solutions for heat equation are discussed as well as the impact of sheath boundary conditions on the continuity of the temperature profile. The nonlocal heat flux is compared to Spitzer-Härm heat flux for different collisionality.

1 Introduction

At the entrance of the scrape-off layer, the plasma collisionality $\nu^\star$ defined as the ratio between the field line length and collision mean free path is found to be of order unity. Despite this low collisionality, tokamak edge plasma modelling relies mostly on the fluid approach and collisional closures that are theoretically only valid at high collisionality. Departure between Braginskii fluid description and kinetic modelling have been highlighted, in particular an underestimation of temperature gradient by the fluid approach [4]. Several kinetic corrections have been proposed to improve plasma description at intermediate collisionality [1,3,6,7]. We investigate in this contribution kinetic corrections to the local Spitzer-Härm (Braginskii) closure for the heat flux; more precisely, we focus on applying the nonlocal expression for the heat flux proposed by Luciani-Mora-Virmont [8] to scrape-off layer physics. We adapt in particular boundary conditions and implement the nonlocal expression into a 1D hydrodynamic model for the scrape-off layer.

2 Nonlocal formulation for heat flux

In order to introduce long range features to the heat flux, we plan to use in this contribution the nonlocal expression for the heat flux expressed in Equation 1. This formulation has been proposed in a broad range of references including [2,4,8].

$$q_{NL}(x) = \int q_{SH}(x')w(x,x')dx' \tag{1}$$

where q_{SH} denotes the Spitzer-Härm expression for the heat flux:

$$q_{SH}(x) = -\kappa(x)\nabla_\parallel T(x) = -\kappa_0 T(x)^{5/2}\nabla_\parallel T(x) \tag{2}$$

and $w(x,x')$ is a kernel describing the space correlation between the temperature gradient and the heat flux. Here, the kernel is an exponential decay, Equation 3, where the decay length is given by the collision mean free path.

$$w(x,x') = \frac{1}{2\lambda(x')}\exp\left(-\frac{|\int_{x'}^{x} n(x'')dx''|}{n(x')\lambda(x')}\right) \tag{3}$$

* Corresponding author E-mail: hugo.bufferand@cea.fr

This kernel tends to a Dirac centered on x for high collisionality i.e. when $\lambda \to 0$. In this case, one recovers the local Fourier law. For flat density profiles and neglecting the temperature dependence upon the mean free path, the kernel $w(x, x')$ reduces to

$$\tilde{w}(x, x') = \frac{1}{2\lambda} \exp\left(-\frac{|x - x'|}{\lambda}\right) \tag{4}$$

In this case, the nonlocal heat flux given by Equation 1 can be re-written in the form of a convolution product of Spitzer-Härm heat flux and an exponential kernel, see Equation 5.

$$\tilde{q}_{NL}(x) = \int \frac{1}{2\lambda} \exp\left(-\frac{|x - x'|}{\lambda}\right) q_{SH}(x')dx' = (\tilde{w} * q_{SH})(x) \tag{5}$$

In order to emphasize the behavior of such a nonlocal expression for the heat flux, let us compute analytical solutions for the heat equation $\partial_x \tilde{q}_{NL} = S$ in a periodic 1D domain. We solve the equation in the Fourier space, $q(x) = 1/2\pi \int_{-\infty}^{\infty} \hat{q}(k)e^{ikx}$, the Fourier transform of the convolution product being the product of the Fourier transforms:

$$\begin{aligned} ik\mathcal{F}[\tilde{q}_{NL}] &= \mathcal{F}[S] \\ \kappa k^2 \mathcal{F}[\tilde{w}]\mathcal{F}[T] &= \mathcal{F}[S] \end{aligned} \tag{6}$$

where we neglected the dependence of the temperature on κ. The Fourier transform of the exponential kernel is given by a Lorentzian:

$$\mathcal{F}[\tilde{w}] = \frac{1}{1 + \lambda^2 k^2} \tag{7}$$

Reporting in Equation 6 gives

$$\mathcal{F}[T] = \left(\frac{1}{\kappa k^2} + \frac{\lambda^2}{\kappa}\right) \mathcal{F}[S] \tag{8}$$

Back to the real space, one finds

$$T(x) = T(0) + x \cdot \left(\partial_x T(0) - \frac{\lambda^2}{\kappa} \partial_x S(0)\right) - \left(\frac{1}{\kappa} \int_0^x dx' \int_0^{x'} dx'' S(x'')\right) + \frac{\lambda^2}{\kappa} S(x) \tag{9}$$

The temperature profiles is thus obtained by summing the double integration of the source (high collisional diffusive behavior) and the source itself ponderated by λ^2/κ. The last term can be neglected at high collisionality. At low collisionality when λ is not zero, the shape of the source is recovered in the temperature profile and if the source is not continuous (e.g. punctual sources modeled as Dirac distributions), neither is the temperature profile. Figure 1 shows temperature profiles for punctual source and sink $S(x) = \delta(x - x_h) - \delta(x - x_c)$ for different value of the collisionality. At low collisionality, the temperature profile is continuous. An analytic solution is also found with continuous gaussian sources. In this case, the solution is continuous at any collisionality. From this analytical analysis, one finds that the nonlocal formulation for the heat flux does not guaranty the continuity of the temperature profile. However, as long as the source is continuous (which is the case in most applications), so is the temperature profile. What about the continuity when adding non-periodic boundary conditions which is necessary for an application to the plasma scrape-off layer?

3 Boundary conditions

3.1 Heat equation with Dirichlet boundary conditions

In order to study the continuity of the temperature profile for a tokamak SOL application. Let us consider first a simple application to the nonlocal heat flux expression to a finite 1D domain of length $L_\parallel$ with Dirichlet boundary conditions:

$$\begin{cases} \partial_x \tilde{q}_{NL} = 0 \\ T(0) = T_{\text{hot}} \quad \text{and} \quad T(L_\parallel) = T_{\text{cold}} \end{cases} \tag{10}$$

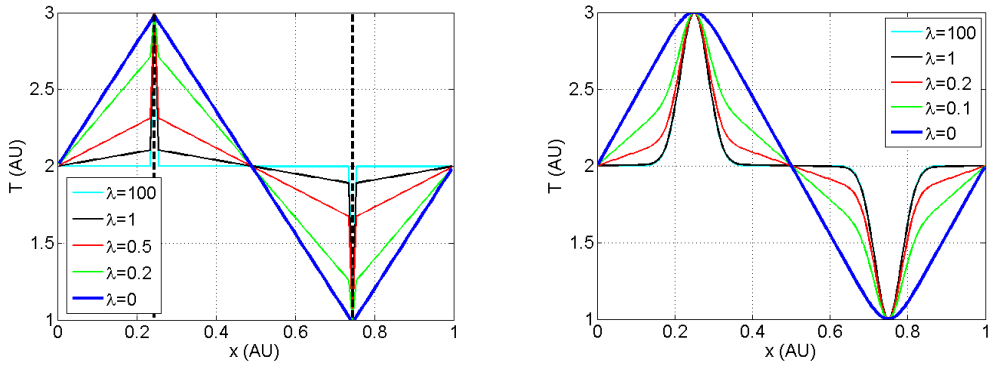

Fig. 1 Temperature profiles obtained by solving heat equation with simplified nonlocal heat flux expression and punctual (left) and gaussian (right) heat source and sink.

Assuming a constant temperature gradient ($\partial_x T = \alpha$) and reporting in the nonlocal heat flux expression, one finds:

$$\begin{aligned} \tilde{q}_{NL}(x) &= -\int_0^{L_\parallel} \frac{1}{2\lambda} \exp\left(-\frac{|x-x'|}{\lambda}\right) \kappa\alpha dx' \\ &= \frac{\alpha\kappa}{2}\left[\exp\left(-\frac{x}{\lambda}\right) + \exp\left(-\frac{L_\parallel - x}{\lambda}\right) - 2\right] \end{aligned} \tag{11}$$

In order to obtain a constant heat flux consistant with $\partial_x q = 0$, one needs to complete the temperature gradient so as to cancel the two exponential functions in Equation 11. This is made possible by adding dirac functions:

$$\partial_x T = \alpha(1 + \lambda\delta_0(x) + \lambda\delta_{L_\parallel}(x)) \tag{12}$$

One finds with this temperature gradient expression $q = -\alpha\kappa$. The temperature is obtained by integrating Equation 12 and considering boundary conditions:

$$T(x) = T_{\text{hot}} + \alpha(x + \lambda H(x) + \lambda H(x - L_\parallel)) \tag{13}$$

where $H(x)$ denotes the Heaviside function. The value of α is found evaluating Equation 13 in $L_\parallel$:

$$\alpha = \frac{T_{\text{cold}} - T_{\text{hot}}}{L_\parallel + 2\lambda} \tag{14}$$

Solutions are plotted for different values of λ on Figure 2. Like with the punctual sources, one finds once again that the temperature profile is not continuous. The discontinuity appears this time at the domain boundary. In order to use the nonlocal kernel combined with an hydrodynamic approach of the plasma, one needs to guaranty the continuity of the temperature including at the boundary. In the following paragraph, we propose a practical way to treat the sheath boundary condition at the ends of the magnetic field line in order to guaranty the continuity of the temperature profile.

3.2 Nonlocal boundary conditions for the sheath

From the previous section, we observe that the use of non-local expression for the heat flux may lead to discontinuities in the temperature profile at the domain boundary. The temperature can be decomposed as $T = \tilde{T} + T_{BC}$ where $\tilde{T}$ is continuous; by definition, we impose $\partial_x\tilde{T}(0) = \partial_x\tilde{T}(L_\parallel) = 0$. The temperature gradient being expressed by

$$\partial_x T = \partial_x\tilde{T} + \partial_x T_{BC} = \partial_x\tilde{T} + \partial_x T(0)\delta(x) + \partial_x T(L_\parallel)\delta(x - L_\parallel) \tag{15}$$

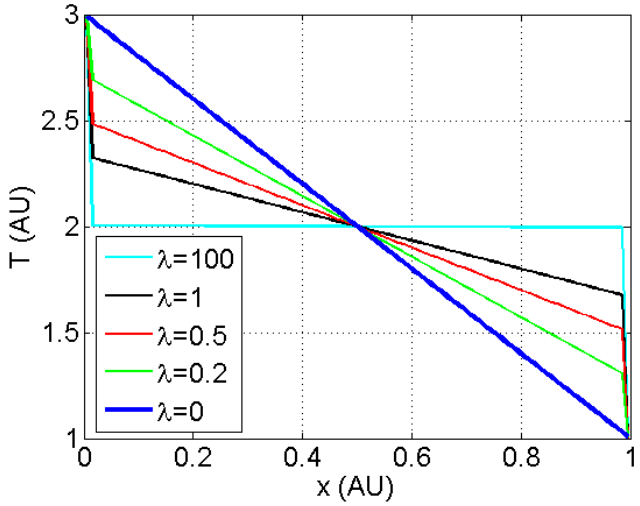

Fig. 2 Analytical solution to the heat equation with the simplified nonlocal expression for the heat flux in a finite 1D domain with Dirichlet boundary conditions. The solutions are plotted for different values of the mean free path λ.

Reporting Equation 15 in the nonlocal expression for the heat flux gives

$$q_{NL,T}(x) = q_{NL,\tilde{T}}(x) + q_{BC,0}\exp\left(-\frac{x}{\lambda}\right) + q_{BC,L_\parallel}\exp\left(\frac{x-L_\parallel}{\lambda}\right) \tag{16}$$

This expression exhibits a first term describing the nonlocal heat flux computed from the continuous temperature gradient $\partial_x\tilde{T}$ in the plasma. The two last terms represent the impact of the boundary condition in the heat flux, effect that decays exponentially away from the wall on a typical length given by the collisional mean free path. The values $q_{BC,0}$ and $q_{BC,L_\parallel}$ are adjusted to match the sheath boundary condition for the heat flux, namely $q_{se} = \gamma n v_\parallel T$ at both ends where γ is the so called sheath transmission coefficient. One has thus at both ends of the field line:

$$\gamma n(0)v_\parallel(0)T(0) = \tilde{q}_{NL,\tilde{T}}(0) + q_{BC,0} + q_{BC,L_\parallel}\exp\left(-\frac{L_\parallel}{\lambda}\right) \tag{17}$$

$$\gamma n(L_\parallel)v_\parallel(L_\parallel)T(L_\parallel) = \tilde{q}_{NL,\tilde{T}}(L_\parallel) + q_{BC,0}\exp\left(-\frac{L_\parallel}{\lambda}\right) + q_{BC,L_\parallel} \tag{18}$$

that is denoting $\nu^\star = L_\parallel/\lambda$ and $\beta = \exp(-\nu^\star)$:

$$q_{BC,0} = \frac{q_{se}(0) - \tilde{q}_{NL,\tilde{T}}(0) - \beta\left(q_{se}\left(L_\parallel\right) - \tilde{q}_{NL,\tilde{T}}(L_\parallel)\right)}{1-\beta^2} \tag{19}$$

$$q_{BC,L_\parallel} = \frac{q_{se}(L_\parallel) - \tilde{q}_{NL,\tilde{T}}(L_\parallel) - \beta\left(q_{se}(0) - \tilde{q}_{NL,\tilde{T}}(0)\right)}{1-\beta^2} \tag{20}$$

4 Application to 1D SOL modelling

The nonlocal model with the above mentioned sheath boundary condition is applied to simulate a 1D SOL hydrodynamic. The following system of Equations is solved for mass, parallel momentum, ion and electron energy

balance:

$$\begin{cases} \partial_t n + \vec{\nabla}\cdot\left(nv_\parallel\vec{b}\right) = S_n \\ \partial_t(m_i n v_\parallel) + \vec{\nabla}\cdot\left(m_i n v_\parallel^2\vec{b}\right) = -\nabla_\parallel p_i + qnE_\parallel \\ \partial_t\left(\frac{3}{2}nT_i + \frac{1}{2}m_i n v_\parallel^2\right) + \vec{\nabla}\cdot\left(\left[\frac{5}{2}nT_i + \frac{1}{2}m_i v_\parallel^2\right]v_\parallel\vec{b}\right) + \vec{\nabla}\cdot\left(q_{i\parallel}\vec{b}\right) = qnv_\parallel E_\parallel - \frac{3}{2}\frac{n}{\tau_{ei}}(T_i - T_e) + S_{Ei} \\ \partial_t\left(\frac{3}{2}nT_e\right) + \vec{\nabla}\cdot\left(\frac{5}{2}nT_e v_\parallel\vec{b}\right) + \vec{\nabla}\cdot\left(q_{e\parallel}\vec{b}\right) = -env_\parallel E_\parallel - \frac{3}{2}\frac{n}{\tau_{ei}}(T_e - T_i) + S_{Ee} \end{cases} \tag{21}$$

where $E_\parallel = -(\nabla_\parallel p_e)/(en)$. The following boundary conditions apply:

$$\begin{cases} \text{Neumann :} & \nabla_\parallel n(0) = \nabla_\parallel n(L_\parallel) = 0 \\ \text{Bohm :} & v_\parallel(0) \le -\sqrt{\frac{T_e(0)+T_i(0)}{m_i}} \quad \text{and} \quad v_\parallel(L_\parallel) \ge \sqrt{\frac{T_e(L_\parallel)+T_i(L_\parallel)}{m_i}} \\ \text{Sheath heat flux :} & q_{i(e)\parallel} = \left(\gamma_{i(e)} - \frac{5}{2}\right)nT_{i(e)}v_\parallel \quad \text{at 0 and } L_\parallel \text{ location} \end{cases} \tag{22}$$

where $\gamma_i = 2.5$ and $\gamma_e = 4.5$. First, simulations are run with a fixed and homogeneous particle source $S_n(x) = S_n^0$. The energy source is also taken homogeneous ($S_{Ee,i}(x) = S_{Ee,i}^0$) and the intensity of the energy source is scanned to change plasma temperature and thus plasma collisionality. Figure 3 shows electron temperature profiles computed for different collisionalities and using different expressions for the heat flux:

- Spitzer-Härm: $q = q_{SH} = -\kappa_{SH}\nabla_\parallel T$
- Flux limited Spitzer-Härm: $q = q_{FL} = \left(q_{SH}^{-1} + q_{max}^{-1}\right)^{-1}$ with $q_{max} = \alpha m_e n c_e^3$ where $c_e = \sqrt{T_e/m_e}$ and $\alpha = 0.15$
- Non-local heat flux $q = q_{NL}$

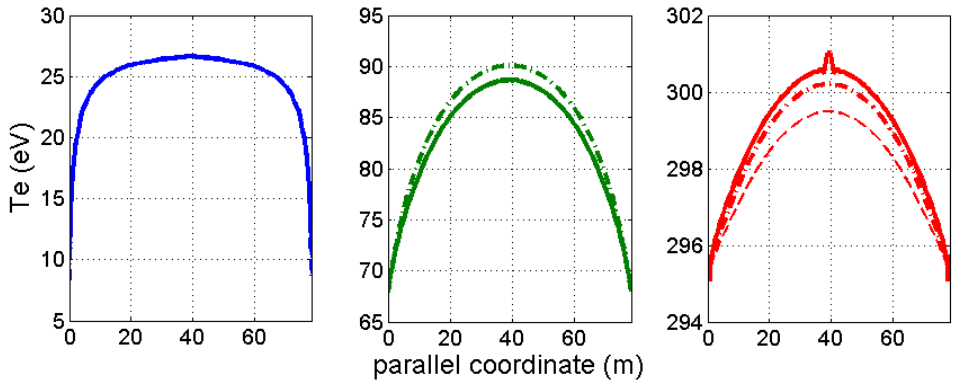

Fig. 3 Electron temperature profiles for different heat flux expressions (solid line: nonlocal, dashed line: Spitzer-Härm, dot-dashed line: Flux limited Spitzer-Härm). The particle and energy sources are homogeneous.

To go further and see the impact of the shape of the source, we now consider a particle source located close to the ends of the field line to simulate recycling:

$$S_n(x) = S_n^0\left[\exp\left(-\frac{x}{0.1L_\parallel}\right) + \exp\left(-\frac{L_\parallel - x}{0.1L_\parallel}\right) + 0.005\right] \tag{23}$$

For the energy sources, we use Gaussian shaped sources located at the middle of the field line. The width of the energy source is controled by λ_E.

$$S_{Ee,i} = S_{Ee,i}^0 \exp\left(-\left(\frac{x}{\lambda_E} - \frac{L_\parallel}{2\lambda_E}\right)^2\right) \tag{24}$$

Figure 4 shows simulation results for $\lambda_E = 0.1L_{\|}$. Once again, the intensity of the source is ramped to change the collisionality.

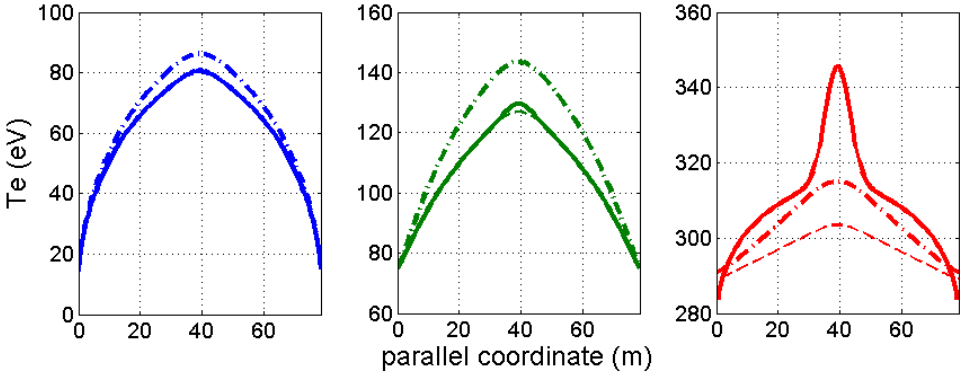

Fig. 4 Electron temperature profiles for different heat flux expressions (solid line: nonlocal, dashed line: Spitzer-Härm, dot-dashed line: Flux limited Spitzer-Härm). The particle and energy sources are peaked.

5 Discussion

On Figure 3 and Figure 4, for high and medium collisonality, there is almost no difference in the temperature profiles obtained considering either the nonlocal expression or the Spitzer-Härm expression. At medium collisionality noticeable effect of the flux limiter leads to increasing temperature gradients for the same heat flux. This leads to an increase of the upstream temperature. Such an increase of the upstream temperature is not observed using the nonlocal heat flux. Figure 5 shows electron heat fluxes calculated from the electron temperature profile obtained at high collisionality with the nonlocal heat flux. One finds a relatively good agreement between the different heat flux expressions, in particular between Spitzer-Härm and the nonlocal expression. All heat flux expressions gives values much below the maximum heat flux value plotted in red as $q_{\max} = 0.15 q_{FS}$ with the free streaming heat flux beging given by $q_{FS} = n_e m_e c_e^3$ with $c_e = \sqrt{T_e/m_e}$.

The situation is more interesting at lower collisionality. The effect of the nonlocal heat flux is more pronounced, in particular when considering peaked sources. On Figure 4, it can be noticed that the temperature profile obtained with the nonlocal heat flux expression shows the superposition of the shape of the sources (temperature peak in the middle of the field line as well as temperature drop close to the wall due to the plasma energy dilution induced by the particle source) on top of a more standard temperature decay that is observed considering diffusive expression for the heat flux. This superposition of the diffusive solution and the source shape was already found analytically in Equation 9. Figure 5 compares heat flux values computed as a post-treatment from the electron temperature profile obtained at low collisionality with peaked sources and with the nonlocal heat flux expression. Unlike the nonlocal expression, one notices that Spitzer-Härm expression gives value way above $q_{\max}$. The nonlocal heat flux expression plays thus actively as a flux limiter. Likewise, one notices obviously that the flux limited Spitzer-Härm heat flux takes value below $q_{\max}$, that is the purpose of the flux limited expression. However, when comparing nonlocal heat flux with local flux limited Spitzer-Härm, one observes a different shape of heat flux, the nonlocal expression exhibiting long range effect of the strong temperature gradient near the energy source. This effect is reminiscent to what is observed in laser heated plasma where the heat source is localised [8]. Localised heat sink near the wall can also drive these strong temperature gradient as observed in [4].

6 Conclusions and perspectives

Using nonlocal heat flux for electron conduction seems to make possible to recover strong temperature gradients and long range interactions at intermediate collisionality. The heat flux is found to be lower than the maximum

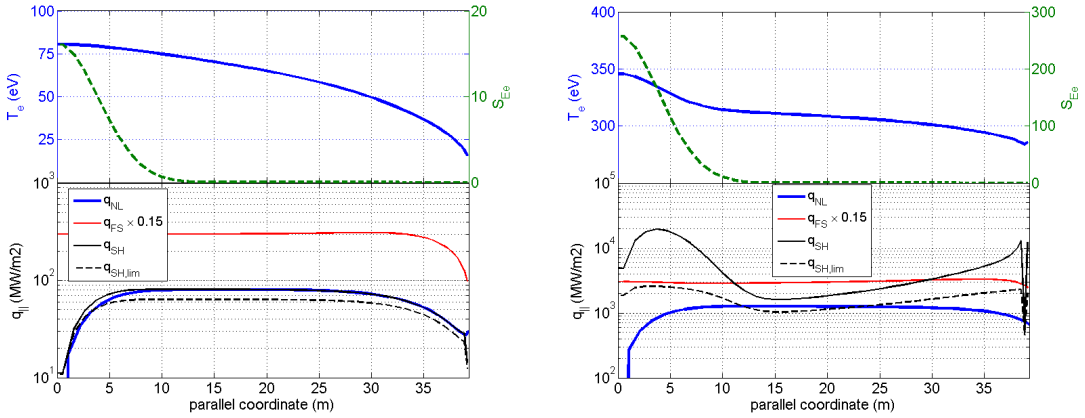

Fig. 5 Comparison of heat flux computed as a post-treatment from the electron temperature profile obtained at low collisionality with the nonlocal heat flux expression and with flat (left) and peaked (right) sources.

free-streaming heat flux. Future comparisons with kinetic PIC simulations [5, 9] should confirm or contradict results obtained with the nonlocal expression.

Acknowledgements

This work was granted access to the HPC resources of Aix-Marseille Universit financed by the project Equip@Meso (ANR-1-EQPX-29-01) of the program "Investissments d'Avenir" supervised by the Agence Nationale pour la Recherche. This work has been carried out within the framework of the EUROfusion Consortium and has received funding from the Euratom research and training programme 2014-2018 under grant agreement No 633053 for the project WP17-ENR-CEA-01. The views and opinions expressed herein do not necessarily reflect those of the European Commission.

References

[1] J.P. Brodrick, R.J. Kingham, M.M. Marinak, M.V. Patel, A.V. Chankin, J.T. Omotani, M.V. Umansky, Del Sorbo D., B. Dudson, J.T. Parker, G.D. Kerbel, M. Sherlock, and Ridgersn C.P. Testing nonlocal models of electron thermal conduction for magnetic and inertial confinement fusion applications. *Phys. Plasma*, 2017.
[2] H. Bufferand, G. Ciraolo, Ph. Ghendrih, S. Lepri, and R. Livi. Particle model for nonlocal heat transport in fusion plasmas. *Phys. Rev. E*, 2013.
[3] A.V. Chankin and D.P. Coster. On the locality of parallel transport of heat carrying electrons in the sol. *J. Nucl. Materials*, 2017.
[4] R. Chodura. Kinetic effects in the scrape off layer. *Contrib. Plasma Phys.*, 1992.
[5] J.P. Gunn. Kinetic investigation of a collisonless scrape-off layer with a source of poloidal momentum. *J. Nuclear Mat.*, 2005.
[6] Yu.L. Igitkhanov and A.M. Runov. Non-local boundary conditions for fluid equations. *Contrib. Plasma Phys.*, 1992.
[7] A.S. Kukushkin and A.M. Runov. Implementation of non-local transport model into 2d fluid code. *Contrib. Plasma Phys.*, 1994.
[8] J.F. Luciani and P. Mora. Nonlocal heat transport due to steep temperature gradients. *Phys. Rev. Letters*, 1983.
[9] D. Tskhakaya. Kinetic modelling of the plasma recombination. *Contrib. Plasma Phys.*, 2016.